Nonlinear Reflection from a Phase-Matched Liquid near the Critical Angle*

PAUL P. BEY, JOHN F. GIULIANI, AND HERBERT RABIN
Naval Research Laboratory, Washington, D. C. 20390
(Received 13 January 1969)

A study of nonlinear reflection in third order is reported. A Q-switched pulse from a neodymium laser at 1.06 μ is internally reflected from a liquid whose refractive index is tuned by the anomalous dispersion of a dye additive. The dye-liquid system is fuchsin red dissolved in hexafluoroacetone sesquihydrate. An increase of more than two orders of magnitude in the intensity of reflected third-harmonic radiation is observed near the critical angle for total internal reflection when the dye concentration is adjusted for phase matching. The experimental third-harmonic data are in good qualitative agreement with theoretical prediction. A comparison is also presented of the shift in phase expected from theory for linear and nonlinear reflection.

I. INTRODUCTION

FOLLOWING the initial demonstration of second-harmonic generation (SHG) by Franken *et al.*,[1] the production of harmonics employing laser radiation has been the subject of extensive experimental and theoretical study.[2] The important role of phase matching has been described,[3,4] and harmonic studies have been extended to third-harmonic generation (THG).[5,6]

Bloembergen and Pershan[7] were the first to give a theoretical description of the interesting case of the generation of harmonics by reflection from a nonlinear medium, and other theoretical works dealing with this general subject have also been carried out.[8–10] The reader is referred to a number of experimental studies of nonlinear reflection and the additional references cited therein.[11–14]

The present paper stems from work reported by Bloembergen and Lee[14] on the generation of reflected second-harmonic radiation in an internal reflection experiment. It was shown experimentally that SHG in reflection at the critical angle is strongly dependent on the degree of phase matching which exists in a nonlinear reflecting medium, and this phenomenon was well accounted for by the earlier theoretical formulation of the reflection problem.[7] The work was carried out using crystals of $NaClO_3$ and KH_2PO_4, the former providing an example of the mismatched case, the latter phase-matched at the critical angle.

The work reported here is an extension of the Bloembergen-Lee experiment to third order, following a preliminary account given in an earlier Letter.[15] Nonlinear reflection is observed from an isotropic liquid medium, hexafluoroacetone sesquihydrate (HS) with additions of the dye fuchsin red; this system was particularly attractive for study in that its refractive index can easily be adjusted by the anomalous dispersion of the dye additive.[16–18] Thus, third-harmonic reflection may be studied in the same medium continuously through the condition of phase matching, i.e., both in the region of normal dispersion as well as anomalous dispersion. Unlike the case of phase matching using birefringence, phase matching in an isotropic medium employing anomalous dispersion is independent of the direction of laser propagation through the medium. Thus, third-harmonic reflection in such a system can be investigated under prescribed phase-matched or mismatched conditions quite independent of the angle of incidence of the laser beam.

Before discussing the experimental measurement of the intensity of internally reflected third-harmonic radiation from the above-mentioned liquid-dye system, the theoretical expression for the intensity is given in Sec. II A. Although experiments are not performed in this work on the phase of the reflected third-harmonic wave, a theoretical determination of the nonlinear phase shift on reflection is also presented (Sec. II B).

* A preliminary discussion of this work was presented at a meeting of the Optical Society of America; see J. Opt. Soc. Am. **58**, 1566 (1968).

[1] P. A. Franken, A. E. Hill, C. W. Peters, and G. Weinreich, Phys. Rev. Letters **7**, 118 (1961).

[2] A comprehensive review has been given by R. W. Minck, R. W. Terhune, and C. C. Wang, Appl. Opt. **5**, 1595 (1966).

[3] J. A. Giordmaine, Phys. Rev. Letters **8**, 19 (1962).

[4] P. D. Maker, R. W. Terhune, M. Nisenoff, and C. M. Savage, Phys. Rev. Letters **8**, 21 (1962).

[5] P. D. Maker, R. W. Terhune, and C. M. Savage, in *Proceedings of the Third International Congress of Quantum Electronics*, edited by P. Grivet and N. Bloembergen (Columbia University Press, New York, 1964), p. 1563.

[6] P. D. Maker and R. W. Terhune, Phys. Rev. **137**, A801 (1965).

[7] N. Bloembergen and P. S. Pershan, Phys. Rev. **128**, 606 (1962).

[8] S. S. Jha, Phys. Rev. **140**, A2020 (1965).

[9] R. Fischer, Phys. Status Solidi **19**, 747 (1967).

[10] J. B. Langworthy, Naval Research Laboratory Report No. 6562, 1968 (unpublished).

[11] R. K. Chang and N. Bloembergen, Phys. Rev. **144**, 775 (1966).

[12] C. C. Wang and A. N. Duminski, Phys. Rev. Letters **20**, 668 (1968).

[13] N. Bloembergen, R. K. Chang, S. S. Jha, and C. H. Lee, Phys. Rev. **174**, 813 (1968).

[14] N. Bloembergen and C. H. Lee, Phys. Rev. Letters **19**, 835 (1967).

[15] P. P. Bey, J. F. Giuliani, and H. Rabin, Phys. Letters **28A**, 89 (1968).

[16] P. P. Bey, J. F. Giuliani, and H. Rabin, Phys. Rev. Letters **19**, 819 (1967).

[17] R. K. Chang and L. K. Galbraith, Phys. Rev. **171**, 993 (1968).

[18] P. P. Bey, J. F. Giuliani, and H. Rabin, J. Quantum Electron. **4**, 932 (1968).

II. THEORY

A. Reflected Third-Harmonic Intensity

The theory of reflection from an isotropic medium has previously been developed by Bloembergen and Pershan.[7] Necessary expressions for the specific case of THG can be directly obtained from their work. The physical situation is depicted in the ray diagram of Fig. 1, where the various propagating wave vectors are drawn in accord with the theoretical analysis of the problem. In a manner analogous to that used in the previous study of SHG by total reflection,[14] the laser beam is considered to be incident from a dense linear medium and then internally reflected by a less dense nonlinear medium.

Both media in the present case are isotropic, and the xy plane in the figure marks the interface between the linear medium of index n_a in the positive z direction and the nonlinear reflecting medium of index n_b along negative z. The linear reflection process at the interface is pictured at the left of Fig. 1, and for clarity the nonlinear process is shown to the right by a displacement of the z axis. The electric and magnetic fields of the incident laser wave are designated $\mathbf{E}_1^i$ and $\mathbf{H}_1^i$, and its wave vector is $\mathbf{k}_1^i$. The incident electric vector is oriented in the plane of incidence, thus corresponding to a transverse magnetic (TM) wave. The reflected and transmitted laser waves are similarly described by $\mathbf{E}_1^R$, $\mathbf{H}_1^R$, $\mathbf{k}^R{}_1$ and $\mathbf{E}_1^T$, $\mathbf{H}_1^T$, $\mathbf{k}_1^T$, respectively. The angles of interest are measured from the normal to the surface as indicated in the figure.

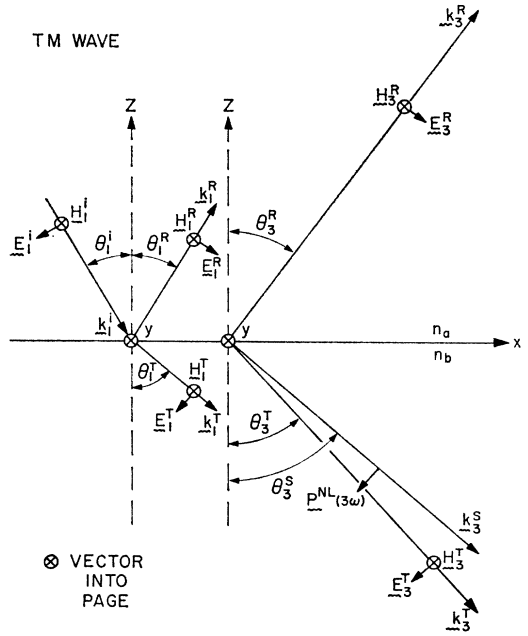

FIG. 1. Linear and nonlinear reflection (the latter displaced to the right for clarity) at the boundary between a linear isotropic medium with refractive index n_a and a nonlinear isotropic medium with refractive index n_b. The plane of polarization of the incident laser wave is taken to correspond to the TM case.

The solution to the linear reflection problem is well known. Continuity of the tangential components of the fields everywhere at the boundary requires equality of the x components of the wave vectors:

$$k_{1x}{}^i = k_{1x}{}^R = k_{1x}{}^T, \tag{1}$$

and Snell's law follows directly:

$$\sin\theta_1{}^T = [n_a(\omega)/n_b(\omega)] \sin\theta_1{}^i. \tag{2}$$

For an internal reflection under consideration here, n_a is larger than n_b, and therefore $\theta_1{}^T > \theta_1{}^i$ as shown in the figure.

The third-harmonic reflected and transmitted waves are shown in the right of Fig. 1. The reflected wave in the medium with index n_a is described by fields $\mathbf{E}_3{}^R$, $\mathbf{H}_3{}^R$ and wave vector $\mathbf{k}_3{}^R$. The angle of nonlinear reflection $\theta_3{}^R$ is not, in general, equal to the angle of linear reflection $\theta_1{}^R$, as will be seen below. In the medium characterized by index n_b there are two propagating waves: a third-harmonic inhomogeneous polarization wave $\mathbf{P}^{\mathrm{NL}}(3\omega)$ with wave vector $\mathbf{k}_3{}^S$ and a third-harmonic homogeneous wave with fields $\mathbf{E}_3{}^T$, $\mathbf{H}_3{}^T$ and wave vector $\mathbf{k}_3{}^T$. The inhomogeneous wave is generated by the transmitted laser wave $\mathbf{E}_1{}^T$ and, accordingly, propagates in a direction $\theta_3{}^S$ equal to $\theta_1{}^T$. Its wave vector is directly obtained from the wave vector of the transmitted fundamental wave

$$\mathbf{k}_3{}^S = 3\mathbf{k}_1{}^T. \tag{3}$$

The homogeneous wave is the third-harmonic wave at the interface, which is refracted at an angle $\theta_3{}^T$ corresponding to the index at the third-harmonic frequency. The magnitudes of the third-harmonic wave vectors are given in terms of the appropriate refractive indices, and also (for later use) the dielectric constants, by

$$(c/3\omega)k_3{}^R = n_a(3\omega) = \epsilon_R{}^{1/2}, \tag{4}$$

$$(c/3\omega)k_3{}^T = n_b(3\omega) = \epsilon_T{}^{1/2}, \tag{5}$$

$$(c/3\omega)k_3{}^S = n_b(\omega) = \epsilon_S{}^{1/2}. \tag{6}$$

The analytic expressions for reflected and transmitted harmonic waves have been derived[7] [see Eqs. (2.5)–(2.6)], and these expressions are easily modified for THG. In a manner analogous to the linear case represented in Eq. (1), the boundary conditions applied to the third-harmonic waves require that

$$3k_{1x}{}^T = k_{3x}{}^S = k_{3x}{}^T = k_{3x}{}^R. \tag{7}$$

The wave vectors in Fig. 1 show these component relationships. The nonlinear generalizations of Snell's law follow from Eq. (7), using Eqs. (2)–(6):

$$\sin\theta_3{}^S = [n_a(\omega)/n_b(\omega)] \sin\theta_1{}^i, \tag{8}$$

$$\sin\theta_3{}^T = [n_a(\omega)/n_b(3\omega)] \sin\theta_1{}^i, \tag{9}$$

$$\sin\theta_3{}^R = [n_a(\omega)/n_a(3\omega)] \sin\theta_1{}^i. \tag{10}$$

The expression for the magnitude of the electric field

of the reflected harmonic wave is a consequence of the matching of the tangential components of the fields referred to above. This is done by Bloembergen and Pershan in their Eqs. (4.10)–(4.12) for the case of the nonlinear polarization in the plane of incidence, and the following expression is obtained:

$$E_3^R=\frac{4\pi P^{\mathrm{NL}}(3\omega)\{1-[(n_b^2(3\omega)+n_b^2(\omega))/n_b^2(3\omega)]\sin^2\theta_3^S\}}{[n_b(3\omega)\cos\theta_3^S+n_b(\omega)\cos\theta_3^T][n_b(3\omega)\cos\theta_3^R+n_a(3\omega)\cos\theta_3^T]},\quad\text{(for TM wave)}\tag{11}$$

where we have substituted the expressions for the dielectric constants given in Eqs. (4)–(6) and employed Eqs. (8) and (10). Also, the direction of the nonlinear polarization $\mathbf{P}^{\mathrm{NL}}(3\omega)$ is perpendicular to $\mathbf{k}_1^T$ (or $\mathbf{k}_3^S$), along the direction of the electric vector $\mathbf{E}_1^T$ generating the nonlinear polarization. The latter is a consequence of the form of the nonlinear polarization in an isotropic medium,[6] $P_j^{\mathrm{NL}}(3\omega)=3C_{1122}E_j(\mathbf{E}\cdot\mathbf{E})$, where C_{1122} is the nonvanishing component of a fourth-rank tensor describing the third-order polarization. In the present case the magnitude of the third-harmonic polarization is given by

$$P^{\mathrm{NL}}(3\omega)=3C_{1122}(E_1^T)^3.\tag{12}$$

The above treatment was developed for the TM wave. An analogous analysis follows for the transverse electric (TE) wave where the electric vector of the laser wave is polarized perpendicular to the plane of incidence. This solution is also given[7] [see Eq. (4.5)], and, using the appropriate third-harmonic expressions in Eqs. (4)–(6), it follows that

$$E_3^R=\frac{-4\pi P^{\mathrm{NL}}(3\omega)}{[n_b(3\omega)\cos\theta_3^T+n_a(3\omega)\cos\theta_3^R][n_b(3\omega)\cos\theta_3^T+n_b(\omega)\cos\theta_3^S]},\quad\text{(for TE wave)}\tag{13}$$

where $P^{\mathrm{NL}}(3\omega)$ is described by Eq. (12), except that E_1^T refers to the magnitude of the electric vector of the transmitted laser wave for the TE case.

The intensity of the reflected third-harmonic radiation follows from the magnitude of the Poynting vector:

$$I^R(3\omega)=(c/4\pi)|E_3^R||H_3^R|=(c/4\pi)n_a(3\omega)|E_3^R|^2,\tag{14}$$

where we have used Eq. (4) in the expression

$$\mathbf{k}_3^R\times\mathbf{E}_3^R=(3\omega/c)\mathbf{H}_3^R$$

to obtain $|H_3^R|$. It is convenient to use the linear Fresnel relations for reflection and refraction,

$$F_1^R=E_1^R/E_1^i,\tag{15}$$

$$F_1^T=E_1^T/E_1^i,\tag{16}$$

and in the nonlinear case to define a third-harmonic Fresnel factor for reflection

$$F_3^R=E_3^R/4\pi P^{\mathrm{NL}}(3\omega).\tag{17}$$

Substitution of Eqs. (12), (16), and (17) into Eq. (14) yields the following expression for the intensity of reflected third-harmonic radiation in terms of the magnitude of the electric field of the incident wave $|E_1^i|$:

$$I^R(3\omega)=36\pi c n_a(3\omega)|C_{1122}|^2|E_1^i|^6|F_1^T|^6|F_3^R|^2.\tag{18}$$

The well-known expressions for the linear Fresnel factors are[19]

$$F_1^T=\frac{2\cos\theta_1^i\sin\theta_3^S}{\sin(\theta_1^i+\theta_3^S)\cos(\theta_1^i-\theta_3^S)},\quad\text{(for TM wave)}\tag{19}$$

and

$$F_1^T=\frac{2\cos\theta_1^i\sin\theta_3^S}{\sin(\theta_1^i+\theta_3^S)},\quad\text{(for TE wave)}\tag{20}$$

where θ_3^S has been substituted for θ_1^T [in accord with the discussion preceding Eq. (3)]. Corresponding expressions for the nonlinear factors[20] are obtained from Eqs. (11), (13), and (17):

$$F_3^R=\frac{1-\{[n_b^2(3\omega)+n_b^2(\omega)]/n_b^2(3\omega)\}\sin^2\theta_3^S}{[n_b(3\omega)\cos\theta_3^S+n_b(\omega)\cos\theta_3^T][n_b(3\omega)\cos\theta_3^R+n_a(3\omega)\cos\theta_3^T]},\quad\text{(for TM wave)}\tag{21}$$

and

$$F_3^R=-\{[n_b(3\omega)\cos\theta_3^T+n_a(3\omega)\cos\theta_3^R][n_b(3\omega)\cos\theta_3^T+n_b(\omega)\cos\theta_3^S]\}^{-1},\quad\text{(for TE wave)}.\tag{22}$$

[19] See, for example, M. Born and E. Wolf, *Principles of Optics* (Pergamon Press, Inc., New York, 1964), p. 40.

[20] In the numerator of Eq. (21) the term in square brackets is divided by $n_b^2(3\omega)$; this was incorrectly transcribed in Eq. (2) of Ref. 15 as $n_b^2(\omega)$. The term involving the linear Fresnel factor in Eq. (18) was inadvertently omitted from Eq. (1) of the previous work and accordingly is not included in the theoretical curves shown in the figure of that reference.

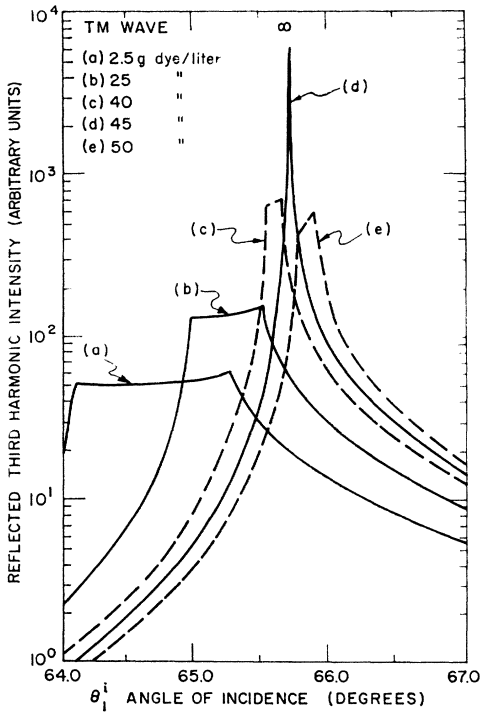

FIG. 2. Theoretical values of intensity of third-harmonic reflected radiation versus angle of incidence of a TM laser wave in the vicinity of the critical angle for total internal reflection. The curves are generated from Eq. (18) in the text, employing the Fresnel factors in Eqs. (19) and (21), the angular relationships in Eqs. (8)–(10), and refractive indices in Table I. These indices correspond to an interface formed by an optically dense solid (fused quartz) and less dense liquid with dye additions (fuchsin in HS) specified in curves (a)–(e).

The intensity function $I^R(3\omega)$ [Eq. (18)] is now completely defined in terms of the angle of incidence of the laser beam $\theta_1{}^i$, for the TM wave by Eqs. (19) and (21), and for the TE wave by Eqs. (20) and (22), using the appropriate angular relationships given in Eqs. (8)–(10).

The singularities present in the nonlinear Fresnel factor near the critical angles have been discussed in the earlier SHG studies.[14] It can be seen from Eqs. (8), (9), and (11) that, when $n_b(\omega)\neq n_b(3\omega)$ corresponding to the phase-mismatched case, the reflected third-harmonic power has two cusps at values of $\theta_1{}^i$ for which $\theta_3{}^S=\frac{1}{2}\pi$ and $\theta_3{}^T=\frac{1}{2}\pi$; for phase matching in the nonlinear medium, $n_b(\omega)=n_b(3\omega)$, it is clear that there is one singularity corresponding to the value of $\theta_1{}^i$ for which $\theta_3{}^S=\theta_3{}^T=\frac{1}{2}\pi$. The value $\theta_3{}^S=\frac{1}{2}\pi$ is associated with total reflection at the fundamental frequency, and $\theta_3{}^T=\frac{1}{2}\pi$ corresponds to total reflection at the third-harmonic frequency.

In Fig. 2 a family of theoretical curves is plotted for the intensity of reflected third-harmonic radiation versus angle of incidence of a TM laser wave in the vicinity of the above-mentioned critical angles. These curves were generated for the media which have been experimentally investigated and are reported upon in Sec. III. The cusp structure mentioned above is clearly evident and so is the critical role of phase matching in the reflecting medium. As the dye concentration is increased sequentially in curves (a)–(d), one passes from the case of the largest mismatch in (a) to perfect matching in (d) (see Table I). In the process, the critical angles coalesce at the point where only one singularity occurs at perfect phase matching, and there is an appreciable associated enhancement of the magnitude of the third-harmonic reflected component. As the dye concentration is further increased [curve (e)], mismatching again occurs and the maximum harmonic intensity is reduced and displaced to higher angles. Note that the index mismatch $\Delta n_b=n_b(3\omega)-n_b(\omega)$ has changed sign in curve (e) from the mismatch in curves (a)–(c).

A comparison of the TM and TE waves is given in Fig. 3 according to predictions of theory. Data are shown reproduced from Fig. 2 for the TM wave, and the corresponding curves for the TE wave are similarly evaluated using Eqs. (20) and (22). There does not appear to be any striking differences in the predicted angular intensity function for the two representative cases selected, the curves in Fig. 3(a) corresponding to phase matching, and the curves in Fig. 3(b) providing examples of mismatching.

B. Phase of Reflected Third-Harmonic Wave

It is well known that in the process of linear reflection there is a phase shift between the incident and reflected waves, and this phase shift is dependent on the angle of incidence. The phase shift Φ_1 is easily determined from Eq. (15) by writing

$$F_1{}^R=|F_1{}^R|e^{i\Phi_1}, \tag{23}$$

and using the well-known linear Fresnel relations for the reflected TM and TE cases[19]

$$F_1{}^R=\frac{\tan(\theta_1{}^i-\theta_3{}^s)}{\tan(\theta_1{}^i+\theta_3{}^s)}, \quad \text{(for TM wave)} \tag{24}$$

and

$$F_1{}^R=-\frac{\sin(\theta_1{}^i-\theta_3{}^s)}{\sin(\theta_1{}^i+\theta_3{}^s)}, \quad \text{(for TE wave)}. \tag{25}$$

TABLE I. Refractive indices at quartz-liquid interface for the neodymium laser and its third harmonic at 20°C.

Medium	Refractive index 1.06 μ	Refractive index 0.353 μ
Fused quartz[a]	$n_a(\omega)$ 1.4490	$n_a(3\omega)$ 1.4760
Fuchsin in HS[b] (g/liter)	$n_b(\omega)$	$n_b(3\omega)$
2.5	1.3030	1.3162
25	1.3125	1.3185
40	1.3185	1.3200
45	1.3205	1.3205
50	1.3225	1.3210

[a] Corning Glass Works fused quartz 7940.
[b] Dye fuchsin red A803, Fisher Scientific Co., dissolved in liquid HS, obtained from E. I. Du Pont de Nemours & Co.

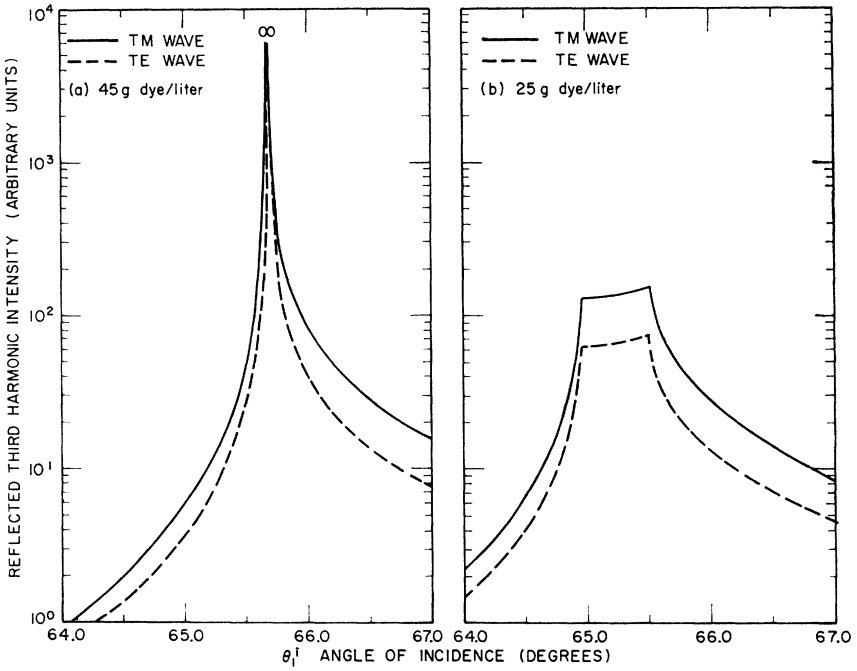

FIG. 3. Comparison of the angular intensity of reflected third-harmonic radiation for TM and TE waves. In (a) and (b) the TM data are identical to corresponding curves (d) and (b), respectively, appearing in Fig. 2. The TE curves are computed in analogous fashion to the TM case, except for the appropriate use of Eqs. (20) and (22).

In a somewhat analogous manner the phase of the reflected wave in the nonlinear problem may be evaluated from the expression obtained by substitution of Eqs. (12) and (16) into Eq. (17):

$$E_3^R/(E_1^i)^3 = 12\pi C_{1122}(F_1^T)^3 F_3^R. \quad (26)$$

In order to avoid the ambiguity inherent in determining the relative phase between waves of different frequency (the incident laser wave and the reflected third-harmonic wave), the nonlinear phase shift for third-harmonic reflection Φ_3 may be defined as the phase of the complex ratio given in Eq. (26). If C_{1122} is taken to be a positive real quantity (as for a lossless nonlinear

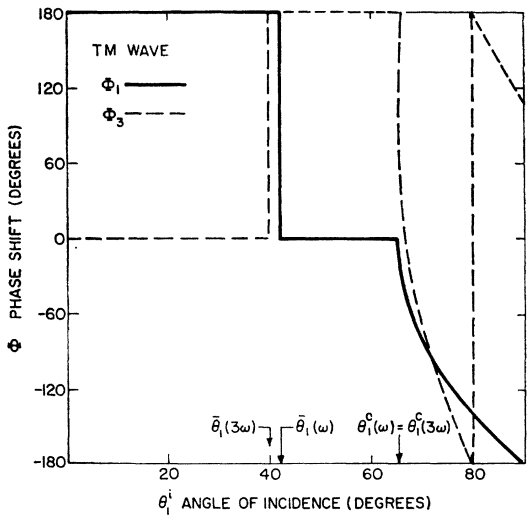

FIG. 4. Theoretical values of linear and nonlinear phase shifts as a function of the angle of incidence of an internally reflected TM laser wave, as determined by Φ_1 and Φ_3, respectively, in Eqs. (23) and (27). Values of Φ_1 were obtained from Eq. (24), upon substitution of refractive index values in Eq. (8). Similarly, Φ_3 was obtained from Eqs. (19) and (21), employing Eqs. (8)–(10). The indicated Brewster and critical angles are defined by Eqs. (28)–(32). Representative refractive index data were used from Table I for quartz and 45-g/liter dye in HS.

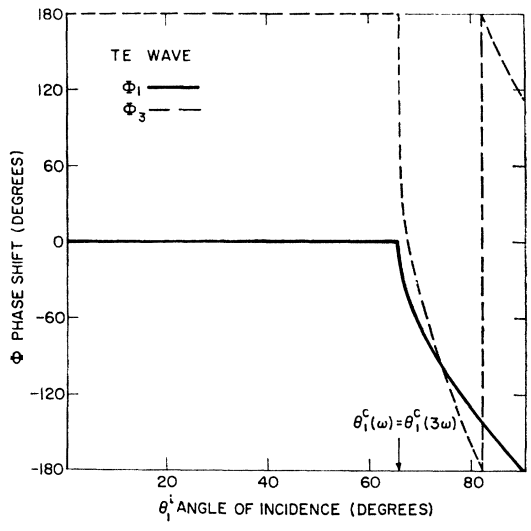

FIG. 5. Theoretical values of linear and nonlinear phase shifts as a function of the angle of incidence of an internally reflected TE laser wave, as determined by Φ_1 and Φ_3, respectively, in Eqs. (23) and (27). Values of Φ_1 were obtained from Eq. (25), upon substitution of refractive index values in Eq. (8). Similarly, Φ_3 was obtained from Eqs. (20) and (22), employing Eqs. (8)–(10). The indicated Brewster and critical angles are defined by Eqs. (28)–(32). The index values used in these plots are the same as stated in the caption of Fig. 4.

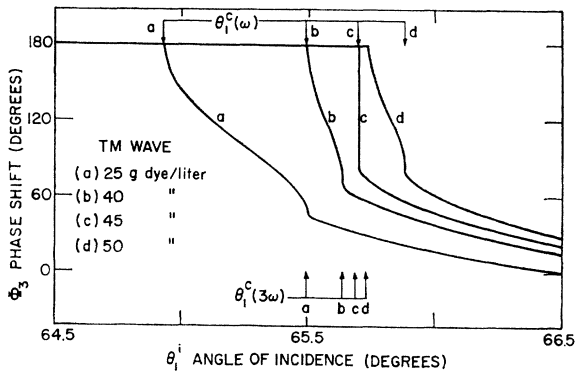

FIG. 6. Theoretical values of nonlinear phase shift as a function of angle of incidence of an internally reflected TM laser wave, as determined by Eq. (27). Φ_3 is obtained from Eqs. (19) and (21), employing Eqs. (8)–(10). The indicated critical angles are defined by Eqs. (31) and (32), and refractive index data for the dye concentrations noted in the figure are obtained from Table I.

isotropic medium), then only the phase need be considered of the product

$$(F_1{}^T)^3F_3{}^R=|F_1{}^T|^3|F_3{}^R|e^{i\Phi_3}, \tag{27}$$

which is directly obtained from the linear and nonlinear Fresnel relations (19)–(22).

In Figs. 4 and 5 the linear and nonlinear phase shifts Φ_1 and Φ_3 are plotted for internally reflected TM and TE waves using refractive index data for the phase-matched case given in Table I. There are clearly appreciable differences in the relative phases in the linear and nonlinear cases.

Figures 4 and 5 show the positions of the Brewster and critical angles and their nonlinear analogs. The (linear) Brewster angle

$$\bar{\theta}_1(\omega)=\tan^{-1}[n_b(\omega)/n_a(\omega)] \tag{28}$$

follows in the usual way from Eq. (2), requiring $\bar{\theta}_1(\omega)=\theta_1{}^i=\frac{1}{2}\pi-\theta_1{}^T$. The nonlinear Brewster angle for third-harmonic reflection $\bar{\theta}_1(3\omega)$ is the value of $\theta_1{}^i$ for which $E_3{}^R=0$ in Eq. (11). Using Eq. (8), the third-harmonic Brewster angle is

$$\bar{\theta}_1(3\omega)=\sin^{-1}\left(\frac{n_b(\omega)n_b(3\omega)}{n_a(\omega)[n_b{}^2(3\omega)+n_b{}^2(\omega)]^{1/2}}\right). \tag{29}$$

For the special case shown in Fig. 4 corresponding to phase matching in the nonlinear medium, $n_b(\omega)=n_b(3\omega)$, the latter value becomes

$$\bar{\theta}_1(3\omega)=\sin^{-1}[n_b(\omega)/\sqrt{2}n_a(\omega)]. \tag{30}$$

The (linear) critical angle $\theta_1{}^c(\omega)$ is the value of $\theta_1{}^i$ for which $\theta_1{}^T=\frac{1}{2}\pi$ as given by Eq. (2):

$$\theta_1{}^c(\omega)=\sin^{-1}[n_b(\omega)/n_a(\omega)]. \tag{31}$$

The nonlinear critical angle for third-harmonic reflection $\theta_1{}^c(3\omega)$ can be defined analogously as the value of $\theta_1{}^i$ for which $\theta_3{}^T=\frac{1}{2}\pi$, and from Eq. (9),

$$\theta_1{}^c(3\omega)=\sin^{-1}[n_b(3\omega)/n_a(\omega)]. \tag{32}$$

Thus, in general, $\theta_1{}^c(\omega)\neq\theta_1{}^c(3\omega)$, except in the special case of phase matching, corresponding to that shown in Figs. 4 and 5. According to expressions (28) and (29), one may similarly obtain a common Brewster angle $\bar{\theta}_1(\omega)=\bar{\theta}_1(3\omega)$.

The phase of the reflected third-harmonic wave shows unique structure for an angle of incidence of the laser wave in the vicinity of the singular points associated with the values of $\theta_1{}^c(\omega)$ and $\theta_1{}^c(3\omega)$ as given by Eqs. (31) and (32). Figure 6 shows the detailed phase shift in the vicinity of these critical angles for both phase-matched and mismatched cases for the TM wave. (Analogous behavior is noted in the TE case, and therefore is not included.) Curve (c) in this figure is an expansion of a portion of the corresponding phase-shift curve shown in Fig. 4 for phase matching, which undergoes a sharp discontinuity at the common critical angle $\theta_1{}^c(\omega)=\theta_1{}^c(3\omega)$. Inspection of Eq. (27), with appropriate substitutions from Eqs. (19) and (21), indicates that there is a discontinuous change in phase of 90° at this common critical angle (where the phase jumps from 180° to 90°). At larger angles of incidence the phase shift decreases monotonically. In the mismatched cases there is no discontinuity of this type, as shown in curves (a), (b), and (d). Here it is observed that the shift in phase only undergoes a change in slope at the separate critical angles $\theta_1{}^c(\omega)$ and $\theta_1{}^c(3\omega)$. It is noted in the curves (a) and (b) for normal dispersion that $\theta_1{}^c(\omega)<\theta_1{}^c(3\omega)$, whereas in curve (d) for anomalous dispersion the opposite inequality is obtained.

III. EXPERIMENTAL

The experimental arrangement is shown diagrammatically in Fig. 7. A laser pulse is incident from the left on a quartz-liquid interface, and the reflected third-harmonic signal generated at the boundary is pictured entering a photodetector. The angle of incidence of the laser pulse $\theta_1{}^i$ and the angle of the reflected third-harmonic $\theta_3{}^R$ are shown in correspondence to the previous discussion of Fig. 1.

The laser was a Korad neodymium glass type K1 with a sapphire resonant output reflector and a KQS2 Pockels cell Q switch. The main portion of the laser beam was reduced optically, prior to passage through a rectangular aperture 1.0×3.0 mm and impingement at the quartz liquid interface. The laser beam was plane-polarized with its electric vector oriented in the plane of incidence at the surface of the liquid; the power density at this point ranged between 30 and 40 MW/cm² and pulse lengths were between 15 and 30 nsec.

Figure 7 shows a top view of the cell configuration used in the experiment. A cylindrical liquid cell with one face removed was cemented on its circumference to the face of a 60° fused-quartz prism. The liquid introduced

into the cell thus provided a plane interface with the surface of the prism which was prepared as a $\frac{1}{2}\lambda$ optical flat. The laser beam entered one of the adjacent surfaces of the prism at near normal incidence, was reflected from the quartz-liquid interface, and made its exit at the third prism surface again at near normal incidence. This configuration allowed for incidence at the angle for total internal reflection at the liquid-quartz boundary. The angle of incidence of the laser beam $\theta_1{}^i$ was varied by use of a spectrometer table (Gaertner model L123), and the small refraction of the laser beam in entering the prism was accounted for in the angular measurements.

The reflected third-harmonic signal was first passed through an optical filter to remove both the laser radiation and extraneous light from the flash lamp. It was then detected by a photomultiplier (Amperex 56TUVP) and displayed on a cathode-ray oscilloscope (Tektronix 585). This oscilloscope was triggered by a second oscilloscope (Tektronix 519), which monitored the laser pulse by use of a glass beam splitter and an ITT photodiode. The magnitude of the third-harmonic pulses was normalized to take into account variations in the magnitude of the laser pulse using a cubic scaling, $I(3\omega) \propto [I(\omega)]^3$.

The prism serves as the optically dense medium for total reflection, and its refractive index is specified by its known composition (Corning Glass Works fused silica 7940). Index values used in this study are given in Table I at the fundamental laser wavelength, 1.06 μ, and its third harmonic at 0.353 μ. The less dense medium is the liquid HS, $(CF_3)_2CO \cdot 1.5H_2O$, with additions of the dye fuchsin red, $C_{22}H_{24}N_3Cl$. Its refractive index values are given in Fig. 8 and also tabulated in Table I for the specific dye concentrations used in these studies.

The index values plotted in Fig. 8 were measured using the technique of minimum angle of deviation by placing the liquid with varying dye concentrations in a hollow prism. The above-mentioned spectrometer table with associated collimator and telescope was outfitted with appropriate photomultipliers at the telescopic eyepiece to make measurements at the wavelengths of interest. The index measurements at 1.06 μ were terminated at a dye concentration of 50 g/liter because of the loss of sensitivity associated with absorption at higher concentrations. The data points follow the solid straight line shown in the figure. Index values at 0.353 μ could not be obtained with the presence of dye in HS, because of the high absorptive loss, so only the single datum for the pure liquid (zero dye concentration) was obtained, using a hollow prism. In order to extrapolate to a higher dye concentration at the third-harmonic wavelength, a second value was taken to correspond to the index at 1.06 μ at the phase-matched dye concentration of 45 g/liter determined in earlier studies.[16–18] The dashed line in Fig. 8 representing the index at 0.353 μ is thus drawn between the measured point at zero dye concentration and the value of the fundamental index at 45 g/liter as inferred from phase matching. The justification for this procedure is left for the later evaluation of the results of this investigation.

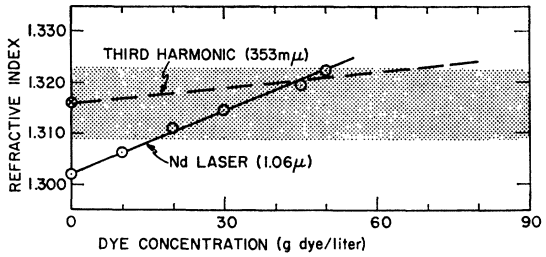

FIG. 8. Refractive index of HS as a function of concentration of additions of the dye fuchsin red. Measurements were made at the neodymium laser line at 1.06 μ over the range 0–50 g/liter, and are represented by the solid line. The dashed line at 0.353 μ is drawn between the measured point at zero dye concentration and the value of index at 1.06 μ for 45-g/liter concentration, corresponding to index matching at the fundamental and third-harmonic frequencies, as previously determined. The measurements at 1.06 μ and the single measurement at 0.353 μ were made in a hollow prism, using the technique of determination of the minimum angle of deviation. The shaded area represents the range of index data at 0.353 μ, obtained by a separate linear reflection measurement from the liquid surface.

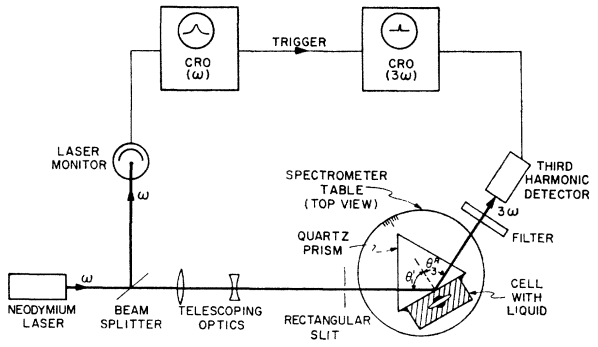

FIG. 7. Diagrammatic representation of the experimental arrangement. The laser radiation at 1.06 μ is monitored by a photodiode, and is displayed on a cathode-ray oscilloscope. The main laser pulse passes through a rectangular aperture before entering the quartz prism for internal reflection at the quartz-liquid interface. Reflected third-harmonic radiation is selectively passed through an optical filter and enters a photomultiplier to be displayed on a second oscilloscope.

It was possible, however, to confirm by an independent measurement that these extrapolated index values at the third-harmonic frequency were reasonable. In Fig. 8 a shaded region is shown corresponding to the uncertainty range of index values at 0.353 μ determined by measuring the linear reflectivity from the surface of liquid HS with dye concentrations to 90 g/liter. These measurements were made on a model 14 Cary spectrophotometer with a reflectance attachment. There is a broad range of agreement between these data and extrapolated values represented by the dashed line in the figure. Because of the appreciable uncertainty of more than 0.01 in the data determined by reflection, they do not in themselves serve as a satisfactory basis for index specification. It is for this reason that the index values in Table I were read to four decimal places from the

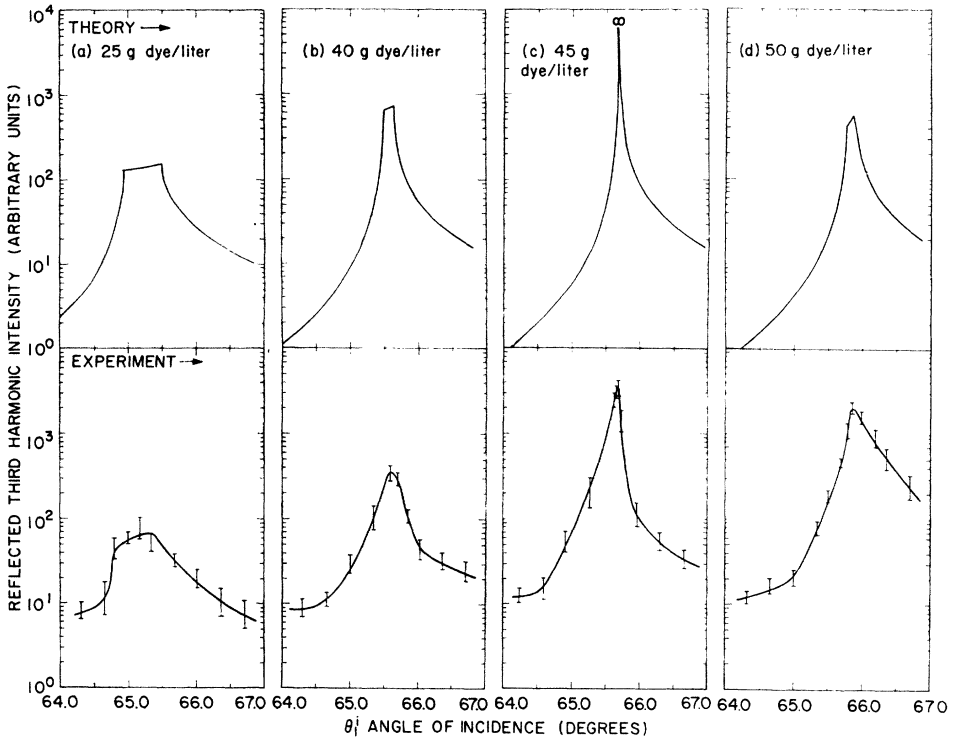

FIG. 9. Comparison of theoretical and experimental values of intensity of third-harmonic reflected radiation versus the angle of incidence of a TM laser wave at a quartz-liquid interface. Variations of dye concentration present in liquid HS are indicated in curves (a)–(d). The theoretical curves have been calculated in the manner indicated in the caption to Fig. 2. Error bars on the experimental curves represent the range of values obtained in approximately five laser shots at each angle.

straight lines of Fig. 8 for use in this study. There is no implication that the values are actually known to this degree of accuracy; they are assumed solely for purposes of the theoretical calculations, which are sensitive to index variations in the fourth place.

In Fig. 9 the experimental results are presented together with corresponding theoretically determined curves for a TM wave. The range of angles of incidence which are plotted are in the vicinity of the critical angles for total internal reflection at the fundamental and third-harmonic frequencies. The theoretical curves were determined by a calculation of the third-harmonic intensity as developed in Eq. (18). The experimental data were obtained in a series of measurements with dye concentrations corresponding to phase matching (45 g/liter), as well as mismatching with $n_b(3\omega)>n_b(\omega)$ at lower concentration (25 and 40 g/liter) and with $n_b(\omega)>n_b(3\omega)$ at higher concentration (50 g/liter). These data, as represented by the error bars, correspond to the range of values obtained in approximately five separate laser shots for each angle of incidence.

IV. DISCUSSION

It has been possible to extend the Bloembergen-Lee experiment to third order because of the relatively large reflected harmonic intensity in the vicinity of the critical angle. This has been mentioned by Lotsch[21] in terms of an enhanced penetration depth of the laser wave close to the critical angle. Figure 10 shows a theoretical plot of reflected third-harmonic intensity over the entire range of angles of incidence of the laser wave from zero to 90° for both TM and TE waves. The intensity is pictured over a 12-decade range, and it is clear that the most satisfactory region to detect third-harmonic reflected radiation is near the critical angle. In particular, the fact that the intensity function near the critical angle is sensitive to phase matching in the nonlinear medium, as shown in the theoretical curves of Figs. 2 and 9, has provided an additional means of verifying the production of reflected harmonic light.

The experimentally determined angular intensity curves compare favorably with the theoretical curves as summarized in Fig. 9. The same general trends are shown in both sets of curves:

(1) There is a narrowing in approaching the phase-matched case with an associated increase in the peak value.

(2) There is a successive shift of the peak to larger angles of incidence in increasing the dye concentration through phase matching (as seen in Fig. 2).

(3) There is a definite asymmetry with a steeper rise for angles of incidence less than the critical angle, and more gradual slope at larger angles.

The principal discrepancy is in the magnitude of enhancement between the wings and peak of the curves. The theoretical curves are considerably more enhanced. Angular divergence of the laser beam would have the effect of reducing the sharpness of the peaks. This divergence could be associated with the beam spread of

[21] H. K. V. Lotsch, J. Opt. Soc. Am. 58, 551 (1968), see Ref. 69.

the laser, a small misalignment of the optics, or diffraction and scattering of the laser beam. Sharp cusplike features of the theoretical curves are not reproduced experimentally; however, this can be attributed both to angular divergence effects as well as to variations in harmonic intensities with spatial and temporal fluctuations in the beam in successive laser shots at different angles of incidence.

It is of interest to compare the intensity of third-harmonic radiation generated by transmission through the nonlinear medium to that obtained by internal reflection at the critical angle. A direct comparison was obtained by use of a simple liquid cell employed previously in transmission studies.[16] This cell was substituted for the reflectance cell shown in Fig. 7 and the third-harmonic intensity was directly measured at the same laser power level as employed in the reflection measurements for a TM wave. Data were obtained at both the phase-matched dye concentration (45 g/liter)as well as for 40 g/liter. The ratio of third-harmonic power generated by transmission to that generated by reflection was approximately 1×10^2 for both dye concentrations. This ratio can be compared to a theoretical estimate using the expression for transmitted third-harmonic intensity previously given[16] and the corresponding expression for the intensity of reflected third-harmonic radiation stated in Eq. (18). In the latter it is important to include a cosine factor for the variation of laser intensity with angle of incidence. A ratio of 25 was obtained from theory for the case of 40 g/liter, providing approximately a factor of 4 discrepancy with the above-stated experimental result. This is most likely associated with factors which contribute to the angular divergence of the laser beam, since measurements in the vicinity of the critical angle would produce an apparent increased ratio by averaging the rapidly changing intensity values at slightly different angles.

Comment on the model assumed in the analysis is in order. The optically dense medium (fused quartz) was taken to be linear while only the less dense liquid was treated as a nonlinear medium. Accordingly, the analysis of Bloembergen and Pershan was directly applied. The rather good agreement between theory and experiment as shown in Fig. 9 supports this approach. There is fundamental justification for treating the quartz as a linear medium for nonlinear reflection near the critical angle. The third-harmonic amplitude produced in the quartz is of the order of $P_a^{NL}(3\omega)/[n_a^2(\omega)-n_a^2(3\omega)]$, while the corresponding expression due to the nonlinear reflection from the liquid is $P^{NL}(3\omega)/[n_b^2(\omega)-n_b^2(3\omega)]$ in the vicinity of the critical angle, where $P_a^{NL}(3\omega)$ is the third-order nonlinear polarization of the quartz (medium a), and $P^{NL}(3\omega)$ refers to the liquid as defined above. The latter term is at least an order of magnitude larger than the former for the media used in the present work. This results from the fact that the third-order susceptibility of the liquid system at a near phase matching has been measured to be approximately three times

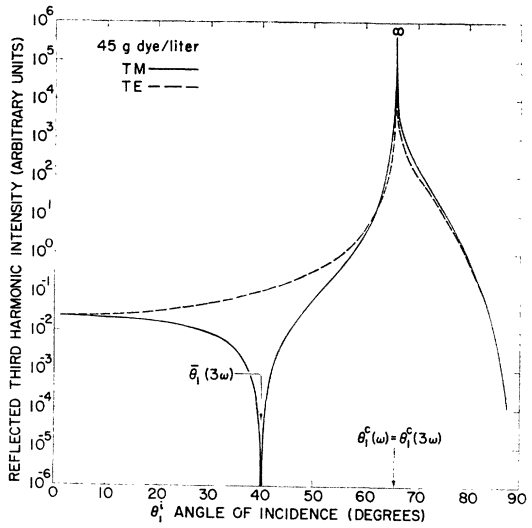

FIG. 10. Theoretical variation of the intensity of third-harmonic reflected radiation as a function of angle of incidence of a laser wave for internal reflection from a nonlinear isotropic medium. Both the TM and TE cases are given, and representative refractive index data are taken from Table I for a quartz-liquid interface with the liquid adjusted for phase matching (45 g/liter). The curves are evaluated from Eq. (18) using appropriate Fresnel factors in Eqs. (19)–(22) and the angular relations in Eqs. (8)–(10).

larger than that of the fused quartz, i.e., $P^{NL}(3\omega)/P_a^{NL}(3\omega)\sim3$, and the ratio of the denominators of the above expressions provides the additional factor at and near phase matching in the liquid. On this basis, the third-harmonic signal generated in the quartz is comparatively small for the near-phase-matched cases examined experimentally, and accordingly the quartz is treated as a linear medium. This is supported by the experimental data presented in Fig. 9, in which only the liquid properties are changed in the sequence of curves (a)–(d), and large changes in reflectivity are observed.

As pointed out in Sec. III, the refractive indices at the third-harmonic frequencies were approximated by a linear extrapolation between the zero and phase-matched dye concentrations. This procedure can now be justified by the general agreement between the experimental and theoretical curves, and particularly the rather good agreement between the values of θ_1^i at which the peak or critical values occur at dye concentrations of 25, 40, and 50 g/liter.

There are two parts of the theoretical analysis which were not evaluated experimentally. First, as shown in Fig. 3, there are differences in the expected angular intensity functions for the TM and TE cases when compared on the same absolute basis. These differences either at phase matching or off phase matching as shown in the figure did not appear to be of sufficient significance to warrant additional measurements for the TE case.

Second, as shown in Figs. 4 and 5, there is appreciable variation between the linear and nonlinear phase shifts on reflection. By adjustment of the phase of the incident laser wave, the phase of the reflected third-

harmonic wave can be altered. Moreover, a wide range of relative phase between the reflected fundamental and harmonic waves may be obtained, depending on the angle of incidence of the laser wave at the interface. Further experimental work might be directed to confirm the unique nonlinear phase shifts which are indicated in the figures, and here an interference experiment[22] could probably be employed in making this determination. In this regard it should be kept in mind that the reflected third-harmonic wave is not coincident with the angle of linear reflection. As shown by Eq. (10), the difference can be appreciable; using the indices for quartz and an angle of incidence $\theta_1^i=66.0°$ for the laser, the harmonic wave is deviated by 2.25° closer to the surface normal.

In Figs. 4 and 5 the usual abrupt changes in phase for linear reflection are apparent at the Brewster and critical angles $\tilde{\theta}_1(\omega)$ and $\theta_1^c(\omega)$, respectively. The analogous third-order Brewster and critical angles $\tilde{\theta}_1(3\omega)$ and $\theta_1^c(3\omega)$ in the figures also provide the demarcation of a sharp change in phase for third-harmonic reflection. The apparent discontinuity of phase at an angle of incidence θ_1^i of approximately 81° shown in Figs. 4 and 5 for the nonlinear case does not carry special significance, since it corresponds to a 2π shift in phase. These data at angles larger than 81° can equally well be joined continuously to the curve at smaller angles by subtraction of 360°. Accordingly, an inspection of the reflected third-harmonic intensity in Fig. 10 in the vicinity of $\theta_1^i=81°$ does not show any abnormalities, unlike the singular behavior on the same plot at both the linear and nonlinear Brewster and critical angles.

In conclusion, the results reported here indicate that concepts of nonlinear reflectivity may be verified in third order. The theoretical treatment in this work follows the lines of development first given by Bloembergen and Pershan[7] and adds further confirmation to their analysis. Moreover, the important role of phase matching in nonlinear reflectivity near the critical angle in second order as shown by Bloembergen and Lee[14] is also present and can be observed in third order as well. The unique feature of the third-harmonic experiments resides in the ability to adjust continuously the same medium for varying degrees of phase matching or mismatching. The results of reflection in third order provide an independent verification of earlier reported work[16] on the production of phase matching using anomalous dispersion. It has also been indicated that the phase of the reflected third-harmonic wave is a function of the angle of incidence of the laser beam, and, accordingly, nonlinear phase shifts may be observed in parallel with similar well-known phenomena encountered in linear reflection.

[22] R. K. Chang, J. Ducuing, and N. Bloembergen, Phys. Rev. Letters 15, 6 (1965).

PHYSICAL REVIEW VOLUME 184, NUMBER 3 15 AUGUST 1969

Augmented-Plane-Wave Virtual-Crystal Approximation*†

J. M. SCHOEN
Department of Electrical Engineering, Columbia University, New York, N. Y. 10027‡
(Received 18 March 1969)

A new perfect-crystal technique based on the augmented-plane-wave (APW) method and the virtual-crystal approximation (VCA) is developed to treat random three-dimensional alloys and partially vacant crystals. The APW VCA is superior to existing perfect-crystal techniques and is a degenerate form of the t-matrix approximation of Korringa and Beeby. An average muffin-tin potential for alloys is proposed. Together with the APW VCA, this model potential can be used to compute band structure and density of states of substitutional alloys. The method of obtaining the density of states from the APW-VCA band structure is more complicated than in perfect crystals.

I. INTRODUCTION

NONSTOICHIOMETRIC compounds and substitutional alloys are very similar to perfect solids. All atoms or vacancies occupy the sites of a lattice; however, equivalent sites are not occupied by equivalent atoms. In a substitutional alloy or nonstoichiometric compound, the set of points at which atoms or vacancies are located shall be defined as the superlattice. Throughout this work, it will be assumed that atoms or vacancies are randomly distributed on this superlattice. The occupation of one site is independent of the occupation of all other sites. Long- or short-range order is therefore precluded. The distinction between substitutional alloys and nonstoichiometric compounds is not essential. Both may be considered as substitutional alloys if we consider the vacancies as generalized atoms. If any class of imperfect solids could be treated by perfect-solid theories, it would appear to be substitutional alloy systems.

* Based on a thesis submitted in partial fulfillment of the requirements for the Ph.D. degree at Columbia University.

† Work supported by U. S. Atomic Energy Commission under Contract No. AT(30-1)3553.

‡ Present address: Bell Telephone Laboratories, Allentown, Pa. 18103.

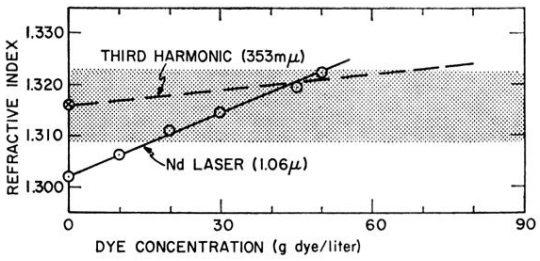

FIG. 8. Refractive index of HS as a function of concentration of additions of the dye fuchsin red. Measurements were made at the neodymium laser line at 1.06 μ over the range 0–50 g/liter, and are represented by the solid line. The dashed line at 0.353 μ is drawn between the measured point at zero dye concentration and the value of index at 1.06 μ for 45-g/liter concentration, corresponding to index matching at the fundamental and third-harmonic frequencies, as previously determined. The measurements at 1.06 μ and the single measurement at 0.353 μ were made in a hollow prism, using the technique of determination of the minimum angle of deviation. The shaded area represents the range of index data at 0.353 μ, obtained by a separate linear reflection measurement from the liquid surface.